FULL PAPER

Dalton
www.rsc.org/dalton

Syntheses, structures, magnetic and spectroscopic properties of bis(pentane-2,4-dionato)chromium(III) complexes incorporating 3- or 4-pyridyl-substituted nitronyl and imino nitroxides†

Atsushi Iino, Takayoshi Suzuki and Sumio Kaizaki *
Department of Chemistry, Graduate School of Science, Osaka University, Toyonaka, Osaka 560-0043, Japan. E-mail: kaizaki@chem.sci.osaka-u.ac.jp

Received 1st September 2003, Accepted 23rd October 2003
First published as an Advance Article on the web 5th November 2003

Preparation and characterization by X-ray analysis and ^{2}H NMR spectra have been described for twelve chromium(III)–nitroxide complexes of *cis*-$[Cr(acac)_2Cl(L)]$ and *cis*- and *trans*-$[Cr(acac)_2(L)_2]PF_6$ with monodentate coordination through the pyridyl-N atom in the nitroxides, where acac = pentane-2,4-dionate and L = 4,4,5,5-tetramethyl-2-(3- or 4-pyridyl)imidazolin-1-oxyl 3-oxide (NIT3py or NIT4py) and 4,4,5,5-tetramethyl-2-(3- or 4-pyridyl)imidazolin-1-oxyl (IM3py or IM4py). An intramolecular magnetic interaction between Cr^{III} and the nitroxide was found to be weakly antiferrromagnetic and ferromagnetic, respectively, in the NIT3py or IM3py complexes and the NIT4py or IM4py complexes. The difference in sign of these magnetic interaction constants between the 3- and 4-pyridyl-substituted nitroxides can be interpreted by a spin polarization mechanism for the π-electron system including the nitroxide SOMO π^* and Cr^{III} d_π orbitals. The inherently weak magnetic interactions and absence of an intensity enhancement of the spin-forbidden d–d transition band in these nitroxides complexes are in contrast to our previous results for the chelated NIT2py [4,4,5,5-tetramethyl-2-(2-pyridyl)imidazolin-1-oxyl 3-oxide] and IM2py [4,4,5,5-tetramethyl-2-(2-pyridyl)imidazolin-1-oxyl] complexes. This may be accounted for by the difference in the mechanism of magnetic interactions; spin-polarization mechanism and exchange mechanism, respectively.

Introduction

Transition metal complexes with nitronyl and imino nitroxides (NIT and IM, respectively) are currently very attractive, because of their potential for usage such as molecular-based ferromagnets and optical devices.[1–4] There have been many magnetic studies for paramagentic[5–7] or diamagnetic metal complexes[8] with NIT2py, NIT3py or NIT4py [4,4,5,5-tetramethyl-2-(2-, 3- or 4-pyridyl)imidazolin-1-oxyl 3-oxide] and IM2py, IM3py or IM4py [4,4,5,5-tetramethyl-2-(2-, 3- or 4-pyridyl)imidazolin-1-oxyl] (Scheme 1), for which a large variation in magnetic properties or mechanism of the magnetic interactions is found to depend on the didenate chelating coordination in 2-pyridyl-substituted nitroxides ($\kappa N^{py}\kappa O^{NIT}$ or $\kappa N^{py}\kappa N^{IM}$)[5] and the monodentate donating one of py-N (κN^{py})[6] or the didentate bridging one of (μ_2-$\kappa N^{py}\kappa O^{NIT}$) in 3- or 4-pyridyl-substituted nitroxides.[7] In order to reveal the coligand effect on the intramolecular metal–nitroxide magnetic interaction as well as the relationships between magnetic and spectroscopic properties or the coordination effect of the nitroxide radicals, we have recently been investigating the magnetic and spectroscopic properties of the NIT2py or IM2py chromium(III), nickel(II) and lanthanide(III) complexes[9–14] and diamagnetic cobalt(III) complexes with NIT3py, NIT4py, IM3py or IM4py,[15] and summarized in the recent review article.[16] In this course, it is invaluable to examine the relation between the magnetic and spectroscopic properties for paramagnetic metal complexes with NIT3py, NIT4py, IM3py and IM4py in comparison with those for the NIT2py and IM2py complexes. Although paramagnetic chromium(III) complexes are found to be suitable to study the relations between the magnetic and spectroscopic properties with variation of coligands or structures as suggested from our previous studies,[9a,11,12] there has been no such monodentate nitroxides Cr(III) complexes other than only one report so far.[17]

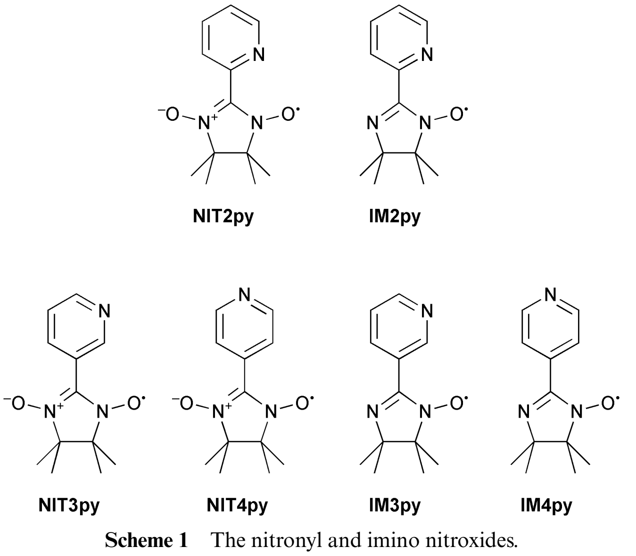

Scheme 1 The nitronyl and imino nitroxides.

Here, we will describe the synthesis, characterization by X-ray analysis and ^{2}H NMR as well as the magnetic and spectroscopic properties for three series of twelve new paramagnetic chromium(III) complexes incorporating monodentate NIT3py, NIT4py, IM3py or IM4py (Scheme 1).

Experimental

Preparation of nitroxides

The nitroxides, NITnpy and IMnpy (n = 3 or 4), were prepared by similar methods to those for the other related nitroxides[15,18] using pyridine-3 or 4-aldehyde. The starting Cr^{III} complex,

---

† Electronic supplementary information (ESI) available: Fig. S1: ORTEP of *trans*-$[Cr(acac)_2(py)_2]^+$ in tpy. Fig. S2: ^{2}H NMR spectra of *m*N3, *m*N4, *m*I3 and *m*I4. Fig. S3: Absorption spectra of pyridine complexes. Fig. S4: UV-vis absorption spectra of *t*I3, *c*I3, IM3py, *t*I4, *c*I4 and IM4py in acetonitrile at room temperature. Fig. S5: The difference absorption spectra of the NIT3py and IM3py complexes from the corresponding pyridine complexes. Fig. S6: The difference absorption spectra of the NIT4py and IM4py complexes from the corresponding pyridine complexes. Fig. S7: Temperature dependence of the magnetic susceptibilities in the form of $\chi_m T$ *vs.* T for *t*N3, *t*N4, *c*I3, *c*I4, *t*I3 and *t*I4. See http://www.rsc.org/suppdata/dt/b3/b310571g/

DOI: 10.1039/b310571g

Table 1 Colour, habits and analytical data (%) of complexes

Compound	Recrystallization solvent	Colour and habit of product	Found (Calc.)		
			C	H	N
***m*N3**·$0.5H_2O$	CH_2Cl_2–C_6H_{14}	Dark blue prisms	49.86 (49.96)	5.83 (5.91)	8.00 (7.94)
***m*N4**	CH_2Cl_2–C_6H_{14}	Green plates	50.46 (50.82)	5.88 (5.82)	7.85 (8.08)
***m*I3**·$0.33H_2O$	CH_2Cl_2–C_6H_{14}	Brown powder	51.78 (51.82)	6.05 (6.06)	8.14 (8.24)
***m*I4**·$0.33H_2O$	CH_2Cl_2–C_6H_{14}	Red powder	51.81 (51.82)	6.15 (6.06)	8.16 (8.24)
***m*py**·$0.2CH_2Cl_2$	CH_2Cl_2–C_6H_{14}	Dark green plates	48.07 (47.39)	5.18 (5.12)	3.63 (3.67)
***t*N3**·H_2O	CH_2Cl_2–Et_2O	Dark blue plates	46.45 (46.31)	5.32 (5.49)	9.53 (9.53)
***c*N3**·CH_2Cl_2	CH_2Cl_2–Et_2O	Dark blue prisms	43.72 (44.31)	4.95 (5.10)	8.73 (8.86)
***t*N4**·$1.5CH_3CN$	CH_3CN–Et_2O	Green powder	48.03 (48.03)	5.51 (5.50)	11.50 (11.35)
***c*N4**·H_2O	CH_2Cl_2–Et_2O	Green powder	46.30 (46.31)	5.40 (5.49)	9.38 (9.53)
***t*I3**	CH_3CN–Et_2O	Orange needles	48.36 (49.10)	5.54 (5.57)	10.22 (10.10)
***c*I3**·H_2O	CH_3CN–Et_2O	Orange powder	46.99 (46.31)	5.63 (5.49)	10.26 (9.53)
***t*I4**·$0.5H_2O$	CH_3CN–Et_2O	Red–brown prisms	48.43 (48.57)	5.50 (5.63)	10.16 (10.00)
***c*I4**·H_2O	CH_2Cl_2–Et_2O	Red microcrystals	46.37 (46.31)	5.38 (5.49)	9.63 (9.53)
***t*py**·$0.5H_2O$	CH_3CN–Et_2O	Red blocks	43.79 (43.41)	4.26 (4.37)	5.21 (5.06)
***c*py**·$1.5H_2O$	$CHCl_3$–Et_2O	Purple microcrystals	42.53 (42.49)	4.30 (4.52)	4.82 (4.95)

trans-[Cr(acac)$_2$(H_2O)$_2$]Cl was prepared by a method described previously,[11,12,19] and the PF_6^- salts were obtained by metathesis with KPF_6 in water. The deuteriated acetylacetonate complexes, *trans*-[Cr(acac-*d*$_7$)$_2$(D_2O)$_2$](Cl or PF_6), were prepared similarly in D_2O using a fully deuteriated acetylacetone [$CD_3C(O)CD_2C(O)CD_3$], which was prepared by refluxing of a mixture of acetylacetone and K_2CO_3 in D_2O for 15 h.[19]

Chloromono(nitroxide) complexes: [Cr(acac)$_2$Cl(L)] (L = NIT3py, NIT4py, IM3py, IM4py and py)

A suspension of *trans*-[Cr(acac)$_2$(H_2O)$_2$]Cl (320 mg, 1.0 mmol) in acetonitrile (50 cm^3) was stirred at room temperature for *ca.* 3 h to give a clear green solution. An equimolar amount (1.0 mmol) of the nitroxide was added to the solution, and the mixture was stirred at room temperature for 1 d. After evaporation of the reaction mixture to dryness under reduced pressure, the residue was extracted with a minimum amount of dichloromethane. Hexane was added to the extract, affording a precipitate of the desired complex, which was collected by filtration, washed with hexane and diethyl ether, and then dried *in vacuo*. Recrystallization was performed from dichloromethane–hexane (Yield for the NIT3py complex: 470 mg, 75%; for the other complexes ~70%). The analytical data were collected in Table 1. The deuteriated acetylacetonate complexes, [Cr(acac-*d*$_7$)$_2$Cl(L)] were prepared similarly from *trans*-[Cr(acac-*d*$_7$)$_2$(D_2O)$_2$]Cl.

Bis(nitroxide) complexes: *trans*- and *cis*-[Cr(acac)$_2$(L)$_2$]PF_6

A mixture of geometrical isomers of *trans*- and *cis*-[Cr(acac)$_2$(L)$_2$]PF_6 was prepared by a similar method to that above with use of [Cr(acac)$_2$(H_2O)$_2$]PF_6 (0.50 mmol) and twice the equimolar amounts (1.0 mmol) of the nitroxide in acetone (50 cm^3). The resulting precipitates of the mixture were dissolved in chloroform (~3 cm^3), and the solution was applied on a recycle preparative HPLC (Japan Analytical Industry Co. Ltd., LP-908 equipped with Jaigel H column), separating into two bands: the faster eluted band (*trans*-isomer) and the slower one (*cis*-isomer). Each eluate was evaporated to dryness, and recrystallized either from acetonitrile, dichloromethane or chloroform–diethyl ether (Yield for the NIT3py complexes: *trans*-isomer, 95 mg, 22%; *cis*-isomer, 75 mg, 17%; for the other complexes: *trans*-isomer, ~20%; *cis*-isomer, ~15%) (Table 1). The deuteriated complexes, [Cr(acac-*d*$_7$)$_2$(L)$_2$]PF_6 were prepared similarly from [Cr(acac-*d*$_7$)$_2$(D_2O)$_2$]PF_6.

Crystallography

The X-ray intensities were measured on a Rigaku automated four-circle diffractometer AFC-5R or AFC-7R [23 °C, graphite monochromated Mo-Kα radiation (λ = 0.71073 Å), the ω–2θ scan mode, $2\theta_{\max} = 60°$]. Absorption corrections were made by an empirical method based on three sets of Ψ-scan data.[20] The structures were solved using SHELXS-86 program and refined on F^2 by full-matrix least-squares using SHELXL-97.[21] All calculations were carried out using a TeXsan software package.[22] The details of each analysis, especially the treatment for the positional disorders, are given below.

A dark blue prismatic crystal of ***m*N3**·$0.5H_2O$ with approximate dimensions of 0.20 × 0.20 × 0.20 mm was grown from dichloromethane–hexane. The O atom of the hydration molecule was located close to the crystallographic center of symmetry, and was treated as a positionally disordered atom with a population of 0.5. For the analysis of ***c*N3**·H_2O (a dark blue prism, 0.20 × 0.10 × 0.10 mm, from acetonitrile–diethyl ether), there were two positions found for the O atom of hydration, but they were too close to be two separate water molecules, so that it was assumed that they were positionally disordered each with a population of 0.5. The compound of ***t*I4**·CH_3CN (a red brown prism, 0.50 × 0.20 × 0.20 mm, from acetonitrile–diethyl ether) crystallized in the triclinic space group $P\bar{1}$ with $Z = 1$; the Cr atom of complex cation and the P of PF_6^- anion were located on crystallographic centres of symmetry. Crystal data are summarized in Table 2.

CCDC reference numbers 218233–218236.

See http://www.rsc.org/suppdata/dt/b3/b310571g/ for crystallographic data in CIF or other electronic format.

Measurements

The magnetic susceptibility data were collected in the temperature range 2.0–300 K and in an applied field 0.2 T with use of a Quantum Design model MPMS SQUID magnetometer. Data were corrected for magnetization of the sample holder and for the diamagnetic contributions, which were estimated from Pascal's constants. Infrared spectra were obtained on a Perkin-Elmer Spectrum GX FT-IR or a Bio-rad FTS-40V spectrophotometer by the Nujol-mull method. UV-vis spectra were measured on a Perkin-Elmer Lambda 19 spectrophotometer. An Oxford liquid helium cryostat model DN1704 and a temperature controller ITC 502 were used for the temperature-dependent measurements of a sample film made from cellulose acetate. The ^2H NMR spectra were recorded on a JEOL Lambda 500 spectrometer at 30°C; chemical shifts are given in the δ scale relative to D_2O.

Results and discussion

Syntheses of the complexes

A clear green solution which was afforded after stirring a suspension of purple [Cr(acac)$_2$(H_2O)$_2$]Cl in acetonitrile probably

Table 2 Crystal data for complexes

Compound	***m*N3**·0.5H_2O	***c*N3**·H_2O	***t*I4**·CH_3CN	***t*py**
Formula	$C_{22}H_{31}ClCrN_3O_{6.5}$	$C_{34}H_{48}CrF_6N_6O_9P$	$C_{36}H_{49}CrF_6N_7O_6P$	$C_{20}H_{24}CrF_6N_2O_4P$
M	528.95	881.75	872.79	553.38
Crystal system	Triclinic	Monoclinic	Triclinic	Tetragonal
a/Å	11.195(2)	25.410(2)	8.785(1)	12.869(1)
b/Å	11.638(3)	13.622(3)	11.135(1)	12.869
c/Å	12.362(2)	12.851(3)	12.071(2)	15.189(1)
α/°	64.44(1)	90	86.20(1)	90
β/°	89.62(2)	95.22(1)	80.83(1)	90
γ/°	67.32(2)	90	80.87(1)	90
U/Å^3	1315.6(4)	4430(1)	1149.9(3)	2515.5(3)
Space group	$P\bar{1}$ (no. 2)	*C*2/*c* (no. 15)	$P\bar{1}$ (no. 2)	$I4_122$ (no. 98)
Z	2	4	1	4
D_c/Mg m^{-3}	1.335	1.322	1.260	1.461
μ(Mo-Kα)/mm^{-1}	0.578	0.373	0.354	0.590
R_{int}	0.024	0.062	0.031	0.009
Refln./param.	7694/307	6467/258	6724/355	1310/86
$R1\{F^2: F^2 > 2\sigma(F^2)\}$	0.043	0.061	0.069	0.047
wR (F^2: all data)	0.130	0.253	0.269	0.165

contained the neutral Cr^{III} complex [Cr(acac)$_2$Cl(H_2O or CH_3CN)]. Addition of the nitroxide, NIT3py, NIT4py, IM3py or IM4py, to the above green solution gave a solution containing *cis*-[Cr(acac)$_2$Cl(nitroxide)] (Scheme 2).

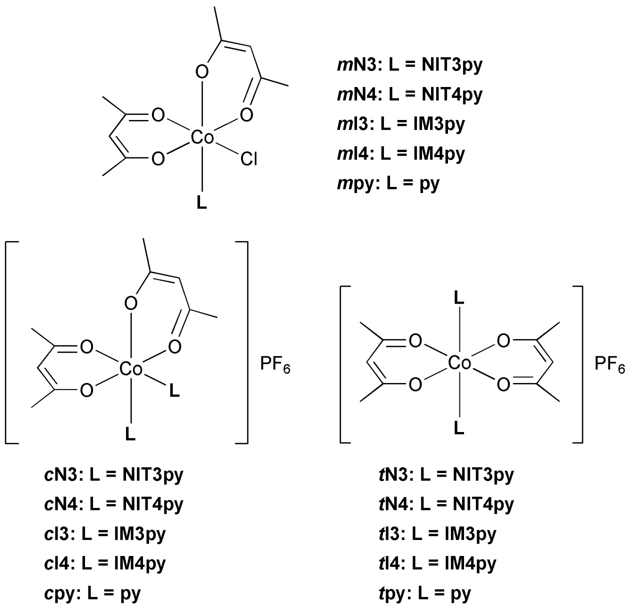

Scheme 2 The complexes prepared in this study.

In order to prepare bis(nitroxide)-type complexes, [Cr(acac)$_2$(H_2O)$_2$]PF$_6$ was used as a starting Cr^{III} complex for the reaction with twice the equimolar amount of the nitroxide in acetone. This reaction gave a mixture of *cis*- and *trans*-[Cr(acac)$_2$(nitroxide)$_2$]PF$_6$ (Scheme 2), which could be separated and isolated with use of a collective HPLC; the faster and slower eluted bands were found to be the *trans*- and *cis*-isomer, respectively (*vide infra*). This synthetic behaviour is contrast to the case of the analogous cobalt(III) NIT3py and NIT4py complexes where the deoxygenation of nitronyl nitroxides occurred to form imino nitroxides.[15]

X-Ray crystal structures

Chloro(nitroxide) complexes. The molecular structure of *cis*-[Cr(acac)$_2$Cl(NIT3py)] (***m*N3**) was determined by X-ray analysis as shown in Fig. 1.

The Cr^{III} ion has an octahedral coordination geometry with a Cl$^-$ and a pyridyl-N bound NIT3py in mutually *cis* positions. Both the bond lengths and angles around the coordinated acac and chloro ligands of Cr(acac)$_2$Cl moiety are typical as compared to those in the related non-radical and non-organometallic complexes.[23,24] The bond lengths and angles around the coordinated NIT3py moiety are comparable to those of the free nitronyl nitroxides such as NIT4py[25] and NIT3,5pym,[26] and those of the coordinated NIT4py in *trans*-[Co(acac)$_2$(PPh$_3$)(NIT4py)]PF$_6$·CH_2Cl_2.[15] The N(1)–O(1) and N(2)–O(2) bond lengths are 1.273(2) and 1.283(3) Å, respectively, suggesting that the radical character of the nitronyl nitroxide is retained in this Cr^{III} complex. The dihedral angle between the nitronyl nitroxide mean plane (O(1)–N(1)–C(7)–N(2)–O(2)) and the pyridyl ring is 40.68(8)°. In this crystal (***m*N3**·0.5H_2O) there are hydrogen-bonding interactions between the nitroxide O(2) and the hydrated water O(10); the distances of O(2) ··· O(10) and O(2) ··· O(10^i) are 2.77(1) and 3.03(1) Å, respectively (symmetry code: (i) $1 - x, 1 - y, 2 - z$).

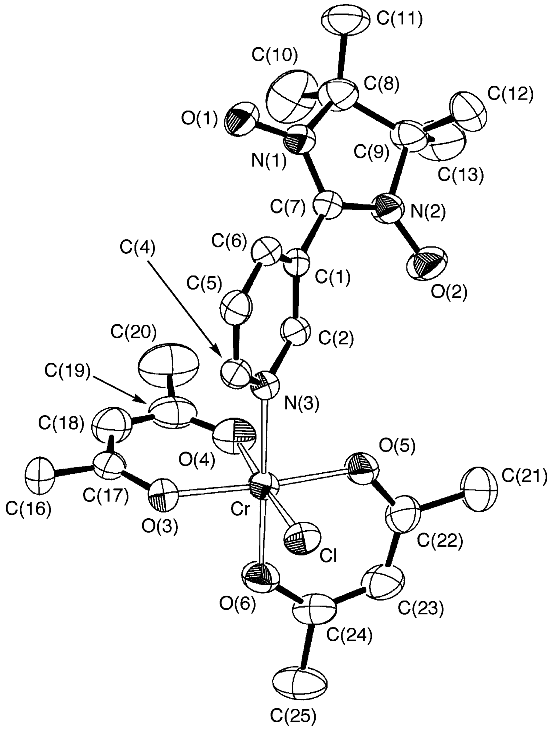

Fig. 1 ORTEP (50% probability level) of [Cr(acac)$_2$Cl(NIT3py)] in ***m*N3**·0.5H_2O. Hydrogen atoms are omitted for clarity. Selected bond lengths (Å) and angles (°): Cr–Cl 2.314(1), Cr–N(3) 2.112(2), Cr–O(3) 1.963(2), Cr–O(4) 1.971(2), Cr–O(5) 1.942(2), Cr–O(6) 1.943(2); O(3)–Cr–O(4) 90.27(8), O(5)–Cr–O(6) 92.11(8).

Bis(nitroxide) complexes. The crystal structures for *cis*-[Cr(acac)$_2$(NIT3py)$_2$]PF$_6$·H_2O (***c*N3**·H_2O), *trans*-[Cr(acac)$_2$-

$(IM4py)_2]PF_6 \cdot CH_3CN$ (***t*I4**·CH_3CN) and *trans*-$[Cr(acac)_2(py)_2]PF_6$ (***t*py**) were characterized by X-ray analysis. The perspective views of the cationic complexes in ***c*N3**·H_2O and ***t*I4**·CH_3CN are shown in Figs. 2 and 3, respectively (that of *trans*-$[Cr(acac)_2(py)_2]^+$ in ***t*py** is given in Fig. S1, ESI †).

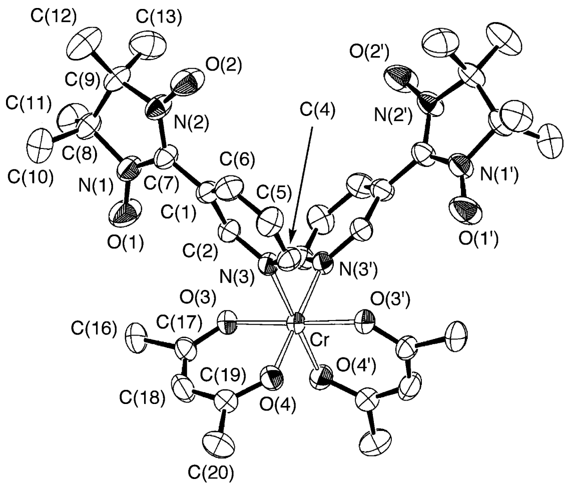

Fig. 2 ORTEP (50% probability level) of the cationic part in ***c*N3**·H_2O (hydrogen atoms are omitted). Selected bond lengths (Å) and angles (°): Cr–N(3) 2.095(4), Cr–O(3) 1.939(3), Cr–O(4) 1.949(4), O(1)–N(1) 1.279(6), O(2)–N(2) 1.280(5); O(3)–Cr–O(4) 91.7(1), N(3)–Cr–N(3′) 88.5(2).

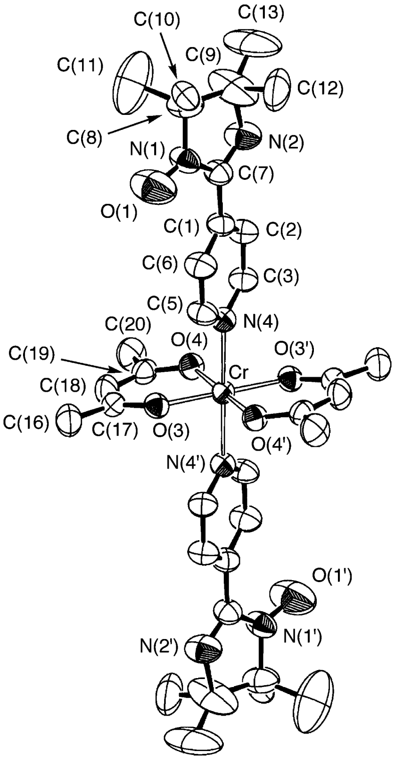

Fig. 3 ORTEP (50% probability level) of the cationic part in ***t*I4**·CH_3CN (for clarity, one set of the disordered imino nitroxide group are shown and all hydrogen atoms are omitted). Selected bond lengths (Å) and angles (°): Cr–N(4) 2.088(3), Cr–O(3) 1.950(3), Cr–O(4) 1.952(3), O(1)–N(1) 1.23(1); O(3)–Cr–O(4) 90.9(1).

For the complexes ***c*N3**·H_2O and ***t*I4**·CH_3CN, two pyridyl-substituted nitronyl or imino nitroxides are coordinated through the pyridyl-N atom to a Cr^{III} center in *cis* and *trans* configuration, respectively. There are no remarkable discrepancies for their structural parameters, as compared to those of the related complexes or free nitroxides[6,8,15,25,26] as well as those of ***m*N3**·$0.5H_2O$.

Table 3 ^2H NMR data of the deuterated acac-d_7 complexes (in CH_3CN, 76.75 MHz, 300 K)

Compound	–CD=	$–CD_3$
m*N3-*d	31.1, 32.1	39.5, 43.2[a]
m*N4-*d	30.2, 32.2	40.4, 44.2[a]
m*I3-*d	29.9, 32.0	39.6, 43.4[a]
m*I4-*d	30.1, 32.0	40.1, 43.7[a]
t*N3-*d	35.7	52.6
t*N4-*d	36.0	54.7
t*I3-*d	35.6	52.5
t*I4-*d	35.5	53.2
t*py-*d	34.6	52.1
c*N3-*d	40.8[a]	46.2[a]
c*N4-*d	41.4[a]	48.2[a]
c*I3-*d	40.6[a]	46.2[a]
c*I4-*d	40.5[a]	46.8[a]
c*py-*d	39.1[a]	45.8[a]

[a] Expected difference in the chemical shifts for the chemically inequivalent methylene-*d* or methyl-d_3 was not detected.

Characterization of the other complexes

The other chloro(nitroxide) complexes, *cis*-[Cr(acac)$_2$Cl(NIT4py, IM3py and IM4py)] (***m*N4**, ***m*I3** and ***m*I4**, respectively) were characterized by far-IR and ^2H NMR spectroscopy. The *ν*(Cr–Cl) bands of ***m*N4**, ***m*I3** and ***m*I4** appeared at 258, 252 and 256 cm^{-1}, respectively, in accordance with that at 266 cm^{-1} for complex ***m*N3**. The ^2H NMR data of the deuteriated acac-d_7 bis(nitroxide) complexes are listed in Table 3. The ^2H NMR spectra of the fully deuteriated ***m*N3-*d***, ***m*N4-*d***, ***m*I3-*d*** and ***m*I4-*d*** were very similar to one another (Fig. S2 of ESI † and Table 3); two or more resonances are observed at *δ* ~37, ~40, ~43 for the methyl deuterons and at *δ* ~30 and ~32 for the methine deuterons. Thus, all of the complexes obtained from a reaction of $[Cr(acac)_2(H_2O)_2]Cl$ and the nitroxide in acetonitrile were characterized as *cis*-[Cr(acac)$_2$Cl(nitroxide-κN^{py})]. The formation of the corresponding *trans*-isomer was not detected in this reaction mixture.

The ^2H NMR spectra of ***t*I4-*d*** and ***t*py-*d***, whose molecular structures were determined by X-ray analysis, showed a resonance at *δ* ~53 for the methyl deuterons and a weak one at *δ* ~35 for the methine deuteron. The complexes of ***t*N3-*d***, ***t*N4-*d*** and ***t*I3-*d*** gave similar spectra, suggesting the same *trans*-bis(nitroxide-κN^{py}) molecular structure for these complexes.[19] In contrast, the ^2H NMR spectra of ***c*N3-*d*** showed a resonance for the methyl deuterons at *δ* 40.8 and a weak one for the methine deuteron at *δ* 46.2. Two resonances for the inequivalent methyl groups in ***c*N3-*d*** were not detected, in contrast to the cases of [Cr(acac-d_6)$_2$(gly)] and [Cr(acac-d_6)(nta)]$^-$.[19] For the *cis* and *trans* isomers, the chemical shifts of the resonances as well as the chemical shift differences between two resonances ($–CD_3$ and –CD=) are different from each other. That is, the methine deuteron in the *trans* isomers gives the higher field resonance than that in the *cis* one, whereas the methyl deuterons in the *trans* isomers give the lower field than that in the *cis* one. Moreover, the differences between *δ*($–CD_3$) and *δ*(–CD=) for the *trans* isomers are larger by about 10 ppm than those for the *cis* one (Table 3). Therefore, such a similar tendency for the ^2H NMR spectra substantiate the assignment of the other bis(nitroxide-κN^{py}) complexes, ***c*N4-*d***, ***c*I3-*d***, ***c*I4-*d*** and ***c*py-*d***, to the *cis* configuration.

UV-vis spectra

The absorption spectra of the nitroxide complexes together with the corresponding pyridine complexes are shown in Figs. 4 and 5 and Figs. S3 and S4 (ESI †).

For the nonradical mono- and bis(pyridine) complexes, ***m*py**, ***c*py** and ***t*py**, the ligand field d–d bands in the visible region were observed, of which the longest wavelength band positions

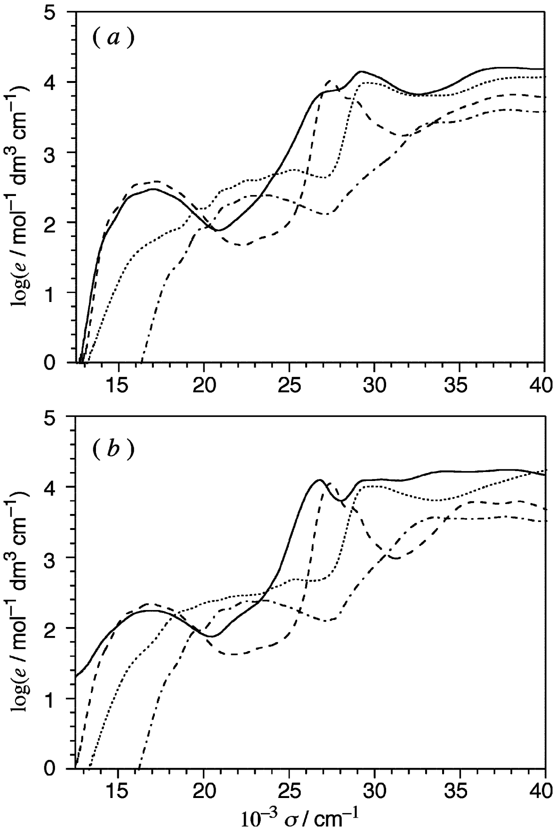

Fig. 4 UV-vis absorption spectra of (a) ***m*N3** (—), ***m*I3** (· · ·), NIT3py (- - -) and IM3py (- · · -); (*b*) ***m*N4** (—), ***m*I4** (· · ·), NIT4py (- - -), and IM4py (- · · -) in acetonitrile at room temperature.

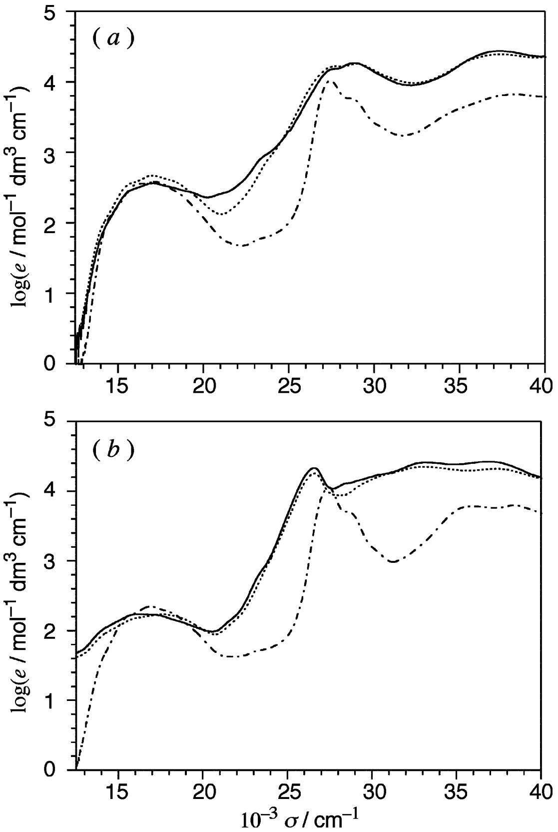

Fig. 5 UV-vis absorption spectra of (a) ***t*N3** (—), ***c*N3** (· · ·) and NIT3py (- · · -); (b) ***t*N4** (—), ***c*N4** (· · ·) and NIT4py (- · · -) in acetonitrile at room temperature.

depend on the chromophore (O_4NCl or O_4N_2 type) and *cis* or *trans* geometrical configurations for nonradical complexes, as usual. However, the higher energy UV bands were very similar to each other (Fig. S3, ESI †). On the other hand, the mono- or bis(NITnpy and IMnpy) complexes showed no ligand-field band in the visible region, but rather broad and/or vibronic bands appeared, which are due to the intraligand NIT n–π* transitions near 17000 cm^{-1} or IM n(NO)–π* transitions near 22000 cm^{-1}. As shown in Figs. 4 and 5, the longest wavelength band for the NIT3py and NIT4py complexes are almost identical in position and intensity with the n–π* band of free NIT3py and NIT4py irrespective of the difference in chromophore or configurations around the Cr^{III} ion. In the UV region where the sharp intense π–π* band for free nitronyl nitroxides (NIT3py and NIT4py) are observed together with a shoulder at higher energy region (~28500 cm^{-1}), there appeared similar bands in intensity and pattern for the corresponding Cr^{III} complexes (Figs. 4 and 5), which are assigned to intraligand π–π* transitions. This π–π* bands for all the NIT4py complexes (***m*N4**, ***c*N4**, and ***t*N4**) were red-shifted by *ca.* 1000 cm^{-1}, while those for the NIT3py complexes (***m*N3**, ***c*N3** and ***t*N3**) were unshifted but became broader. For the imino nitroxide complexes, the similar shift tendency for the n(NO)–π* bands was observed; the red-shift for the IM4py complex, but no shift for the IM3py one. This is confirmed by subtracting the UV-vis spectra of the NITnpy or IMnpy complexes from those of the py complex, which give the perturbed nitroxide's spectrum in the complex (Figs. S5 and S6, ESI †). Such spectral behavior of the NITnpy and IMnpy Cr^{III} complexes is similar to that found in the NITnpy and IMnpy Co^{III} complexes.[15] This difference in perturbation from the NIT4py and IM4py complexes to the NIT3py and IM3py ones is accounted for by the effect of the difference in spin density (and sign) at the pyridyl-N atom.[15]

The variable temperature absorption spectra of the present complexes showed small intensity increases in the n–π* and π–π* transitions with decreasing temperature. In the spin-forbidden d–d transition region where the sharp and weak bands are generally observed near 14000 cm^{-1} for Cr^{III} complexes,[16] the Cr^{III} nitroxide complexes are predicted to show the intensity enhancement as clearly observed for the NIT2py and IM2py complexes.[11,12] However, such an intensity enhancement for the present NIT3py, NIT4py, IM3py and IM4py complexes could not be observed in this region with decreasing the temperature even down to 7 K. Another difference in spectral behavior from the NIT2py and IM2py complexes is the absence of a new metal-to-ligand charge transfer (MLCT) (t_{2g}–SOMO π*) transition in the visible region. This subject will be discussed in connection with the magnetic interactions below.

Magnetic properties

Chloro(nitroxide) complexes. The temperature-dependence of the χ_mT (χ_m = molar magnetic susceptibility) of complexes ***m*N3**, ***m*N4**, ***m*I3** and ***m*I4** are shown in Fig. 6.

For the chloro(nitroxide) complexes, the χ_mT values at 300 K were close to that expected for the independent spin system (S_{Cr} = 3/2 and S_R = 1/2: 2.25 cm^3 K mol^{-1}). On lowering the temperature, however, each complex gave characteristic variable-temperature magnetic susceptibility. For the NIT3py complex (***m*N3**), the χ_mT values decrease gradually on decreasing the temperature, indicating an intramolecular antiferromagnetic interaction between Cr^{III} and NIT3py. At 4.5 K the χ_mT value becomes a minimum (1.38 cm^3 K mol^{-1}) and further lowering the temperature showed an increase of χ_mT. This behaviour may suggest that there is a weaker intermolecular ferromagnetic interaction or a small amount of a paramagnetic impurity contaminated in the sample. For the IM3py complex (***m*I3**), a similar decrease of the χ_mT values on lowering the temperature is also seen probably due to an intramolecular antiferromagnetic interaction.

In contrast to the 3-pyridyl-substituted nitroxide complexes above, the NIT4py and IM4py complexes (***m*N4** and ***m*I4**)

Table 4 Magnetic data of complexes

Compound	g	J/cm^{-1}
***m*N3**	2.00	−2.95
***m*N4**	1.87	5.80
***m*I3**	1.98	−2.07
***m*I4**	1.93	2.11
***t*N3**	1.98	−3.61
***t*N4**	2.05	4.86
***t*I3**	1.84	−1.31
***t*I4**	1.73	3.53
***c*N3**	1.98	−3.02
***c*N4**	2.02	5.65
***c*I3**	1.74	−1.65
***c*I4**	1.94	2.49

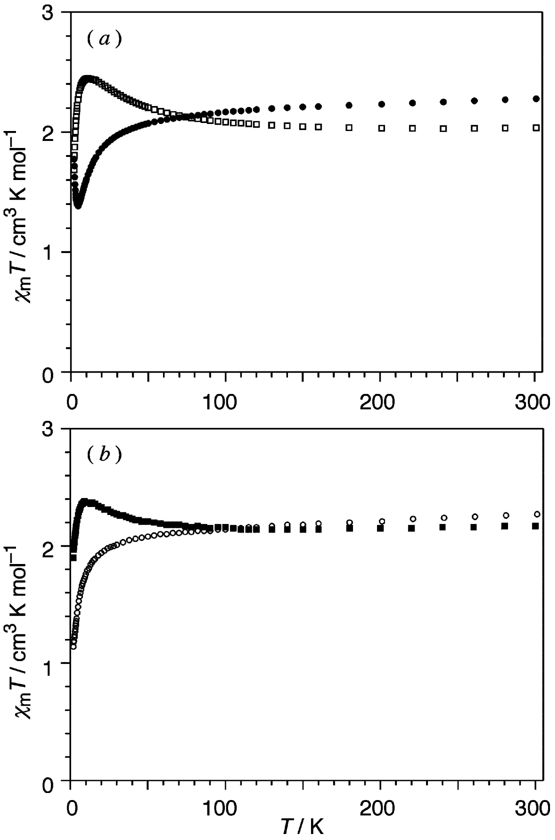

Fig. 6 Temperature dependence of the magnetic susceptibilities in the form of $\chi_m T$ *vs.* T for (a) ***m*N3** (●) and ***m*N4** (□); (b) ***m*I3** (○) and ***m*I4** (■).

showed a different magnetic behavior. Both the complexes gave an increase of the $\chi_m T$ values on lowering the temperature from 300 K, and gave a maximum value at 11 K (2.45 cm^3 K mol^{-1}) for *m*N4 or at 9.0 K (2.38 cm^3 K mol^{-1}) for *m*I4. Further lowering the temperature led to a sharp decrease of the $\chi_m T$ values. These facts suggest that the intramolecular Cr^{III}–nitroxide interaction is ferromagnetic for the 4-pyridyl-substituted nitroxide complexes. The remarkable decrease of the $\chi_m T$ values at lower temperatures would be due either to intermolecular antiferromagnetic coupling or to the zero-field splitting effect of the ground quintet state.

The intramolecular magnetic interaction parameters ($H = -2J S_{Cr} \cdot S_R$) were estimated using eqn. (1).

$$\chi_m = (Ng^2\beta^2/kT)[\{10 + 2\exp(-4J/kT)\}/\{5 + 3\exp(-4J/kT)\}] \quad (1)$$

In order to neglect the possible intermolecular magnetic interaction and the zero-field splitting effect, the data in the range of $T \geq 30$ K are used for the analysis. The estimated results are listed in Table 4.

Bis(nitroxide) complexes. The temperature-dependence of the $\chi_m T$ values of complexes ***c*N3** and ***c*N4** are shown in Fig. 7, and those of the other bis(nitroxide) complexes are given in Fig. S7 (ESI†).

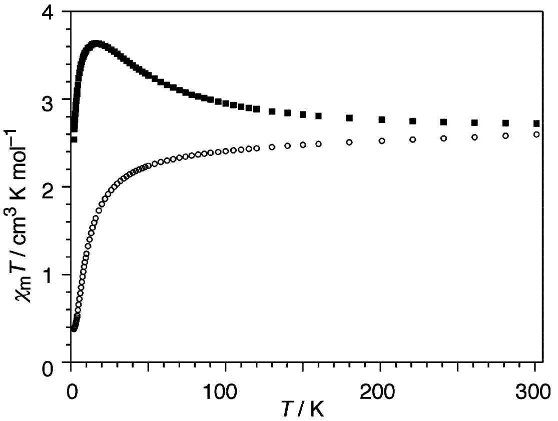

Fig. 7 Temperature dependence of the magnetic susceptibilities for ***c*N3** (○) and ***c*N4** (■) in the form of $\chi_m T$ *vs.* T.

The $\chi_m T$ values of these complexes at 300 K are close to those expected for uncorrelated three spin system. The overall profiles of the temperature-dependency of the susceptibility data of these complexes are similar to those of the mono(nitroxide) complexes, as far as the same nitroxides are concerned. In fact, there is no distinct difference between the geometrical (*cis* and *trans*) isomers, indicating that the intra- and intermolecular nitroxide–nitroxide interaction would be negligibly small for these Cr^{III} complexes.

The intramolecular magnetic interaction parameters [$H = -2J S_{Cr} \cdot (S_{R1} + S_{R2})$] were estimated using eqn. (2), where intramolecular nitroxide–nitroxide interaction ($H' = -2J' S_{R1} \cdot S_{R2}$), intermolecular magnetic interactions, and the zero-field splitting effect were all neglected.

$$\chi_m = \frac{Ng^2\beta^2}{4kT} \cdot \frac{(35 + 10e^{3x} + 10e^{5x} + e^{8x})}{(3 + 2e^{3x} + 2e^{5x} + e^{8x})} \quad (2)$$
$$x = -J/kT$$

The molar susceptibility data with $T \geq 30$ K were used for the analysis, and the obtained parameters are listed in Table 4. The sign and magnitude of the Cr^{III}–nitroxide interaction parameters (J) for these bis(nitroxide) complexes are similar to those for the above chloro(nitroxide) complexes: weakly antiferromagnetic and weakly ferromagnetic for the 3-pyridyl- and 4-pyridyl-substituted nitroxides complexes, respectively. It is worth noting here that a small but reverse influence due to 3- and 4-pyridyl-substituted nitroxides has also been observed for the ^{59}Co NMR chemical shifts of *trans*-[Co(acac)$_2$(NO$_2$)(nitroxide)] and *trans*-[Co(acac)$_2$(PPh$_3$)(nitroxide)]PF$_6$.[15]

General considerations of magnetic interactions

It is difficult to make quantitative comparison in detail among the magnitudes of the J for the present complexes owing to the large deviation of the g values of some of the complexes from typical values of Cr^{III} complexes (Table 4). In three series of complexes, however, there is no remarkable difference in sign and magnitude of the interaction constants between the nitronyl and imino nitroxides of the same substituent (3- or 4-pyridyl group) and among the ligating atmospheres around the Cr^{III} ion (*cis*-ClO$_4$N, *cis*-O$_4$N$_2$ or *trans*-O$_4$N$_2$). The signs of J can be compared with one another in view of the variable-temperature behavior of the $\chi_m T$ as shown in Fig. 6, 7 and S7 (ESI†). Their signs change alternatively with the intervening atoms between the Cr^{III} and the radical moiety in the π-electron system including the nitroxide π* and Cr^{III} d$_\pi$ orbitals just as predicted by a spin-polarization mechanism (Scheme 3). This is evidently substantiated by the fact that the ferro- and antiferromagnetic interactions were found, respectively, for the 3- and 4-(*N*-oxy-*N*-*tert*-butylamino)pyridine (*n*NOpy; *n* = 3 or 4) Cr^{III} complexes, [Cr(TPP or TAP)Cl(nNOpy)] {TPP = *meso*-tetraphenylporphyrinate(2–), TAP = *meso*-tetrakis(methoxyphenyl)-porphyrinate(2–)}.[17] That is, the signs of J for the 3NOpy and 4NOpy complexes are positive and negative, respectively, which are opposite to those of the NIT3py or IM3py and NIT4py or IM4py Cr^{III} complexes. Moreover, the magnitude of J for the NIT3py or IM3py and NIT4py or IM4py complexes ($|J|$ = 2–6 cm^{-1}) are in an order of magnitude smaller than those of the 3NOpy or 4NOpy complexes. Such opposite signs and the diminution in magnitude of J may result from the same causes as for the 4NOpy and NIT4py Mn^{II} complexes as discussed by Iwamura and co-workers;[17] the sign inversion due to one extra intervening bond in NIT4py leading to the different phase of π electron spin-polarization in the pyridine and the difference in magnitude due to a node at the carbon between two nitrogens of NIT.

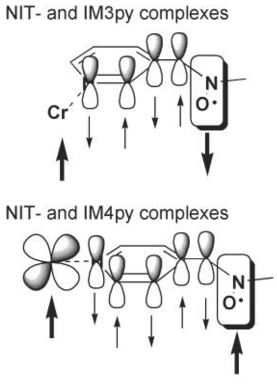

Scheme 3 Spin polarization.

Concluding remarks

The present synthesis and characterization of three series of Cr^{III} complexes with monodenate pyridyl coordination of nitronyl and imino nitroxides allow us to examine their magnetic and spectroscopic properties in comparison with those of the corresponding Co^{III} complexes as well as the chelated NIT2py and IM2py Cr^{III} complexes.

There is some overall similarity in the intraligand n–π* and π–π* absorption spectra between the present nitroxide Cr^{III} complexes and the corresponding Co^{III} complexes. This may provide a clue to elucidate the perturbation from the metal coordination to the intraligand transitions of the nitroxides.

It is interesting to compare the magneto-optical properties of the monodentate NIT3py, NIT4py, IM3py and IM4py Cr^{III} complexes with those of the didentate NIT2py and IM2py Cr^{III} complexes in consideration of the mechanisms of spin-forbidden transition intensity enhancements through the magnetic interactions.

Assuming that the spin-polarization mechanism operates for the NIT2py and IM2py complexes, ferromagnetic interactions were predicted through the pyridyl nitrogen. However, this is not what was found, but only the antiferromagnetic interactions are observed with variation of the β-diketonate coligands in both the NIT2py and IM2py complexes,[11,12] of which the J values for $[Cr(acac)_2(NIT2py\ and\ IM2py)]PF_6$ (*e.g.*, J = −61.6 and −188 cm^{-1}, respectively) are much larger as compared with the NIT3py, NIT4py, IM3py and IM4py Cr^{III} complexes. This is accounted for by the exchange mechanism leading to the variation of the observed magnetic interaction with change of the hypothetical ferromagnetic interaction (J_F) in addition to the constant contribution from the antiferromagnetic interaction (J_{AF}); *i.e.*, $J_{obs} = J_{AF} + J_F$.[11,12] In the previous discussion on the NIT2py and IM2py complexes,[11,12] it was claimed in terms of the exchange mechanism that the constant contribution of J_{AF} are expressed as $(\varepsilon_{SF}/\varepsilon_{CT})\cdot(\Delta E_{CT})^2/(E_{CT})$ where $\varepsilon_{SF}/\varepsilon_{CT}$ is the intensity ratio between the spin-forbidden transition and the MLCT, E_{CT} is the transition energy of MLCT and ΔE_{CT} is the transition energy difference between the spin-forbidden and MLCT, and that the hypothetical J_F may result from the existence of the quintet MLCT state. Other than this contribution, the ferromagnetic interaction due to the spin-polarization mechanism should be taken into consideration. On the other hand, it is likely that the magnetic interaction for the NIT3py, NIT4py, IM3py and IM4py Cr^{III} complexes would predominantly originate from the spin-polarization mechanism; *i.e.*, $J_{obs} = J_{AF}$ for the NIT3py and IM3py or $J_{obs} = J_F$ for the NIT4py and IM4py complexes.

In contrast to the large intensity enhancement of the spin-forbidden d–d transitions in the near infrared region observed for the NIT2py and IM2py Cr^{III} complexes,[11,12] the present Cr^{III} complexes show no enhancement as mentioned before. This is supposed simply due to the small magnitude of J_{obs} as compared with the large one for the NIT2py and IM2py complexes. By considering the exchange mechanism for the magnetic interactions, however, it is seen that the large magnitude of J_{obs} is both required and sufficient for the intensity enhancements, but that the reverse is not true; even for the diminution of J_{obs}, the intensity is enhanced as expected from the constant contribution of J_{AF} irrespective of a large variation of the J_{obs} values for the NIT2py and IM2py Cr^{III} complexes.[11,12] That is, a sufficient condition for the intensity enhancement is not a large magnitude of J_{obs}, but rather the appearance of the MLCT bands due to the large overlap between the SOMO π* and the d_π orbitals that augments the J_{AF} values in terms of the exchange mechanism.[12,16] Thus no observation of the spin-forbidden transition intensity enhancement for the indirect coordinated NIT3py, NIT4py, IM3py and IM4py complexes arises from the absence of the d_π–SOMO π* MLCT, but not necessarily from the small J magnitude as mentioned above.

Acknowledgements

We gratefully acknowledge support of this research by a Grant-in-Aid for Scientific Research (A)(2) (No. 10304056) from the Ministry of Education, Science, Sports and Culture.

References

1 E. Coronado, P. Delhaès, D. Gatteschi and J. S. Miller, *Molecular Magnetism: From Molecular Assemblies to the Devices*, NATO ASI Series 321, Kluwer Academic Publishers, Dordrecht, 1996.
2 (*a*) A. Caneschi, D. Gatteschi, R. Sessoli and P. Rey, *Acc. Chem. Res.*, 1989, **22**, 392; (*b*) A. Caneschi, D. Gatteschi and P. Rey, *Prog. Inorg. Chem.*, 1991, **39**, 331.
3 J. S. Miller, *Inorg. Chem.*, 2000, **39**, 4392 and references therein.
4 K. E. Vostrikova, D. Luneau, W. Wernsdorfer, P. Rey and M. Verdaguer, *J. Am. Chem. Soc.*, 2000, **122**, 718.
5 (*a*) D. Luneau, P. Rey, J. Laugier, E. Belorizky and A. Cogne, *Inorg. Chem.*, 1992, **31**, 3578; (*b*) D. Luneau, G. Risoan, P. Rey, A. Grand, A. Caneschi, D. Gatteschi and J. Laugier, *Inorg. Chem.*, 1993, **32**, 5616; (*c*) K. Fegy, N. Sanz, D. Luneau, E. Belorizky and P. Rey, *Inorg. Chem.*, 1998, **37**, 4518.
6 (*a*) A. Caneschi, F. Ferraro, D. Gatteschi, P. Rey and R. Sessoli, *Inorg. Chem.*, 1990, **29**, 1756; (*b*) A. Caneschi, F. Ferraro, D. Gatteschi, P. Rey and R. Sessoli, *Inorg. Chem.*, 1990, **29**, 4217; (*c*) D. Luneau, F. M. Romero and R. Ziessel, *Inorg. Chem.*, 1998, **37**, 5078.
7 (*a*) F. L. de Panthou, E. Belorizky, R. Calemczuk, D. Luneau, C. Marcenat, E. Ressouche, P. Turek and P. Rey, *J. Am. Chem. Soc.*, 1995, **117**, 11247; (*b*) A. Caneschi, D. Gatteschi, R. Sessoli and P. Rey, *Inorg. Chim. Acta*, 1991, **184**, 67.
8 (*a*) H. Oshio, *Inorg. Chim. Acta*, 2001, **324**, 188; (*b*) C.-J. Lee, C.-H. Huang, H.-H. Wei, Y.-H. Liu, G.-H. Lee and Y. Wang, *J. Chem. Soc., Dalton Trans.*, 1998, 171.

9 (*a*) T. Yoshida, K. Kanamori, S. Takamizawa, W. Mori and S. Kaizaki, *Chem. Lett.*, 1997, 603; (*b*) T. Yoshida and S. Kaizaki, *Inorg. Chem.*, 1999, **38**, 1054; (*c*) T. Yoshida, T. Suzuki, K. Kanamori and S. Kaizaki, *Inorg. Chem.*, 1999, **38**, 1059; T. Yoshida, T. Suzuki, K. Kanamori and S. Kaizaki, *Inorg. Chem.*, 1999, **38**, 5926 (erratum).

10 (*a*) Y. Yamamoto, T. Suzuki and S. Kaizaki, *J. Chem. Soc., Dalton Trans.*, 2001, 1566; (*b*) Y. Yamamoto, T. Suzuki and S. Kaizaki, *J. Chem. Soc., Dalton Trans.*, 2001, 2943.

11 Y. Tsukahara, A. Iino, T. Yoshida, T. Suzuki and S. Kaizaki, *J. Chem. Soc., Dalton Trans.*, 2002, 181.

12 Y. Tsukahara, T. Kamatani, A. Iino, T. Suzuki and S. Kaizaki, *Inorg. Chem.*, 2002, **41**, 4363.

13 Y. Tsukahara, T. Kamatani, T. Suzuki and S. Kaizaki, *Dalton Trans.*, 2003, 1276.

14 T. Tsukuda, T. Suzuki and S. Kaizaki, *J. Chem. Soc., Dalton Trans.*, 2002, 1721.

15 M. Ogita, Y. Yamamoto, T. Suzuki and S. Kaizaki, *Eur. J. Inorg. Chem.*, 2002, 886.

16 S. Kaizaki, *Bull. Chem. Soc. Jpn.*, 2003, **76**, 673.

17 M. Kitano, Y. Ishimaru, K. Inoue, N. Koga and H. Iwamura, *Inorg. Chem.*, 1994, **33**, 6012.

18 (*a*) E. F. Ullman, J. H. Osiecki, D. G. B. Boocock and R. Darcy, *J. Am. Chem. Soc.*, 1972, **94**, 7049; (*b*) T. Akita, Y. Mazaki, K. Kobayashi, N. Koga and H. Iwamura, *J. Org. Chem.*, 1995, **60**, 2092.

19 S. Kaizaki, N. Hirota, C. Tanaka, J. Tano, L. X. Lan and J. I. Legg, *Inorg. Chim. Acta*, 1992, **197**, 185.

20 A. C. T. North, D. C. Phillips and F. S. Mathews, *Acta Crystallogr., Sect. A*, 1968, **24**, 351.

21 (*a*) G. M. Sheldrick, *Acta Crystallogr., Sect. A*, 1990, **46**, 467; (*b*) G. M. Sheldrick, SHELXL-97, University of Göttingen, Germany, 1997.

22 Molecular Structure Corporation and Rigaku Corporation, TeXsan, ver. 1. 11, MSC, The Woodlands, TX, USA, and Rigaku, Akishima, Tokyo, Japan, 2000.

23 B. Morosin, *Acta Crystallogr.*, 1965, **19**, 131.

24 A. G. Orpen, L. Brammer, F. H. Allen, O. Kennard, D. G. Watson and R. Taylor, *J. Chem. Soc., Dalton Trans.*, 1989, S1.

25 (*a*) K. Awaga, T. Inabe and Y. Maruyama, *Chem. Phys. Lett.*, 1992, **190**, 349; (*b*) H.-H. Wei, H.-Y. Wong, G.-H. Lee and Y. Wang, *J. Chin. Chem. Soc.*, 1996, **43**, 253.

26 F. L. de Panthou, D. Luneau, J. Laugier and P. Rey, *J. Am. Chem. Soc.*, 1993, **115**, 9095.